

Three-Dimensional Simulations Capture the Persistent Low-Mode Asymmetries Evident in Laser-Direct-Drive Implosions on OMEGA

A. Colaïtis,¹ I. V. Igumenshchev,² D. H. Edgell,² D. Turnbull,² R. C. Shah,² O. M. Mannion,² C. Stoeckl,² D. W. Jacobs-Perkins,² A. Shvydky,² R. T. Janezic,² A. Kalb,² D. Cao,² C. J. Forrest,² J. Kwiatkowski,² S. P. Regan,² W. Theobald,² V. N. Goncharov,² and D. H. Froula²

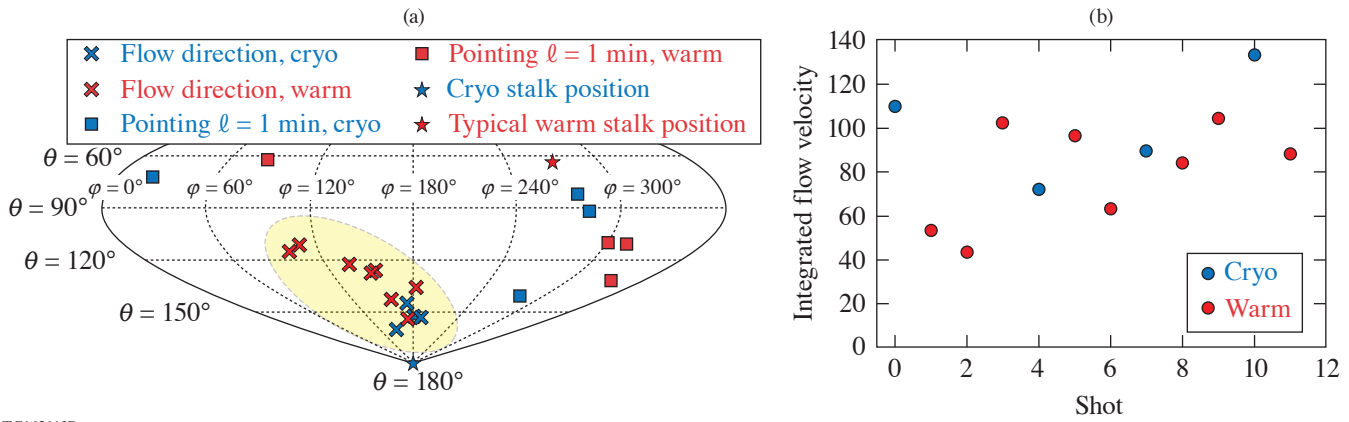
¹Université de Bordeaux, Centre Lasers Intenses et Applications, France

²Laboratory for Laser Energetics, University of Rochester

In this summary, detailed calculations are presented that include the first 3-D hydrodynamic simulations with sufficient physics models included to reproduce and quantify the anomalies observed in direct-drive implosions on OMEGA. When including all the known effects [polarized cross-beam energy transfer (CBET), mispointing, target offset], the simulations reproduce the measurements for bang time, yield, hot-spot flow velocity, and direction. To quantify these effects within the integrated experiments and describe the complex physical processes of polarized CBET and its interplay with multidimensional plasma hydrodynamics, an inline CBET model capable of accounting for polarization was implemented in a 3-D hydrodynamic code with a 3-D laser propagation solver. These integrated simulations were used to assess the effect of unpolarized and polarized CBET, explore the sensitivity of current direct-drive experiments to the various low-mode sources, and assess the predictive capabilities of such detailed 3-D modeling tools—an important component of the inertial confinement fusion program. Notably, current levels of beam mispointing, imbalance, target offset, and asymmetry from polarized CBET were found to degrade yields by more than 40%. Finally, mitigation strategies are explored: attempting to compensate the mode-1 asymmetry with a preimposed target offset and redesigning the double polarization rotators. These results were summarized in Ref. 1 and detailed in Refs. 2 and 3.

For the past few years, direct-drive implosion experiments conducted on the OMEGA Laser System⁴ have reached a sufficient degree of control such that the errors induced by beam power imbalance, beam pointing inaccuracy, and target offset are relatively small. Despite these improvements, a large flow anomaly is still observed across many experiments, with a flow direction that appears systematic⁵ (Fig. 1). Recently, it was proposed in Ref. 6 that a potential source of systematic low modes on the OMEGA laser⁴ originates from polarized CBET. According to the authors of Ref. 6, the polarization dependency of CBET induces a significant low-mode anomaly in the laser drive, with its direction (in terms of spherical harmonics mode $\ell = 1$) being consistent with typical measured flow velocities from neutron diagnostics. Conclusions were reached, however, using post-processing of 1-D hydrodynamics simulations, which do not allow for a quantitative assessment of the final influence of polarized CBET on measured flow velocity and direction, for which inline modeling is required. Moreover, accounting for the compounded effect of beam balance, beam pointing error, and target offset in addition to polarized CBET requires a 3-D modeling of both the laser and hydrodynamics.

This led to the development of the first inline-capable polarized CBET model, implemented within the inverse ray-tracing framework of the *IFRIIT*⁷ code. Inline simulations were performed using a heterogeneous multiple-data, multiple-program framework coupling the *ASTER*^{9,10} 3-D radiation-hydrodynamic code with the *IFRIIT*^{7,10} 3-D laser propagation solver, running on 6000 cores of the French Commission for Atomic Energy and Alternative Energies' Très Grand Centre de Calcul (CEA TGCC) supercomputer, making it possible to describe the complex physical processes of polarized CBET and its interplay with plasma hydrodynamics. These integrated simulations were used to (1) quantify the sensitivity of current target designs to the best setup performances of the OMEGA Laser System, (2) assess if the source of the systematic flow can be identified, and (3) test various strategies for mitigation of the low-mode asymmetries.



TC16211JR

Figure 1

(a) Fusing DT flow direction shown in a sinusoidal projection of the OMEGA chamber and (b) associated flow magnitude in km/s in best-setup implosions (see also Refs. 5 and 11). The yellow region highlights the systematic anomaly.

The inline polarization model proposed here was developed within the field formulation of geometrical ray optics. The ray electric field is written $a = A \exp k_0 \psi$, where k_0 is the vacuum wave number, A is the field swelling due to refraction, and ψ is a phase that includes the effects of absorption and energy exchange. The field at caustics is described using an etalon integral method,¹² which allows reconstruction of the Airy pattern without introducing free parameters. The ray field is then described onto the Frenet reference frame,¹³ an orthogonal basis associated with the ray and defined at every point by a tangent $\mathbf{1} = \mathbf{k} / |\mathbf{k}|$, a normal \mathbf{v} parallel to the permittivity gradient component transverse to the ray, and a binormal $\mathbf{b} = \mathbf{1} \times \mathbf{v}$. The Frenet frame rotates with the ray, which allows for local accounting of polarization transport through refraction. The exchange of amplitude between the ray-field components in the Frenet frame, denoted $(A_n)^T = (a_n, v_n, a_n, b_n)$ for field n , can be written¹³ as $\partial_{1_n} A_n = \underline{D}_n A_n$ with \underline{D}_n a tensor that accounts for three polarization effects: polarization rotation due to refraction, polarization rotation of the probe beam toward the pump beam, and ellipticity induced in the initially linear polarizations due to CBET-induced plasma birefringence.

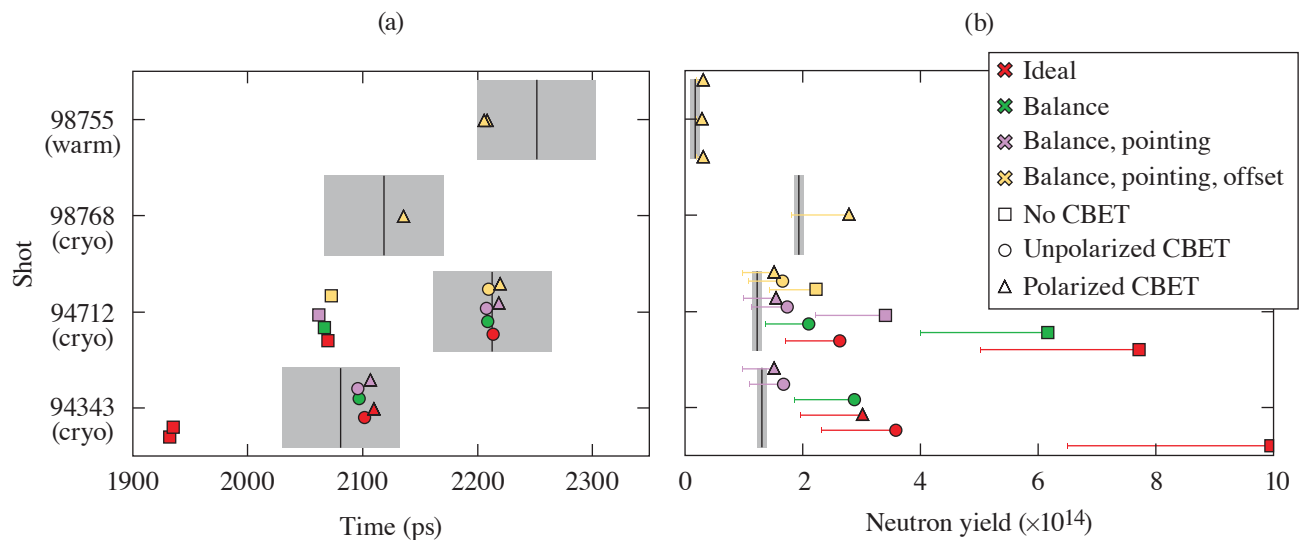
In the final model, the ray amplitude A is computed according to ray theory from a single inverse ray-tracing step,¹⁴ while the ray phase is obtained by integrating the permittivity along the ray trajectory, $\psi = \int e^{\nu} [\mathbf{r}(\hat{\tau}) d\hat{\tau} / 2]$, which includes e^{ν} , the effect of polarized CBET from \underline{D}_n , as well as collisional absorption and Langdon effect.^{10,15} Pump depletion is obtained by iterating the ray phase computation until convergence. The final formulation of the laser propagation model has no free parameters, contrary to what is commonly used in inline CBET models to either limit caustic fields or tune the CBET interaction.¹⁶⁻¹⁹ This polarized CBET model was validated against academic test cases and against the *BeamletCrosser* post-processor^{2,6} and is now used in inline 3-D *ASTER/IFRIIT*^{9,10} simulations. The full polarized CBET model and its validation are presented in Ref. 2.

The 12 shots reported in Fig. 1 span 19 months of operation and were obtained with good performance metrics for beam pointing, beam balance, offset error, target quality, and diagnostic quality. Out of these 12, three shots were modeled; 94343, 98755, and 98768. Among those, 94343 and 98768 are cryogenic shots, whereas 98755 is a warm plastic shot. Shot 98768 is a large-diameter shot with $D_t = 1012 \mu\text{m}$, while the others are smaller targets with $D_t \sim 980 \mu\text{m}$. To this set, we also add shot 94712 (Ref. 11), which was a cryogenic shot with poor pointing performances, contrary to the other three noted above. For these experiments, the beam pointing was measured at the beginning of the shot day. In addition, for shot 98755, pointing was also measured at the end of the shot day, providing two references. Finally, the ice-thickness uniformity was characterized using optical measurements prior to the shots. For the targets of interest, the ice layer nonuniformity was estimated to be less than the instrument resolution, i.e., $<1\%$ for the mode $\ell = 1$.

An extensive set of simulations was executed while varying the CBET model and/or the number of low-mode sources, which are included. The CBET model was toggled from off, to the commonly used unpolarized model²⁰ where the polarization effect for polarization-smoothed beams [e.g., distributed polarization rotation (DPR)] is modeled with fixed polarization and without any

rotation or ellipticity effects to the fully polarized model presented here. In all simulations, the Spitzer–Härm²¹ heat conduction model was used at all times except in the first picket where the flux was limited with $f_{\text{lim}} = 0.1$ (Ref. 8).

The inline simulations are compared to various measurements: peak rise time of the neutron rate, yield, flow velocity magnitude, and direction. Several conclusions can be drawn from the simulations results for neutron data, some of which are reported in Fig. 2: (1) The CBET model alone gets nuclear bang time correctly, implying that the zero-order drive energetics are correct and well described by the model [Fig. 2(a)]. This also suggests that other effects not accounted for here, such as two-plasmon decay, do not significantly modify the total drive.²² (2) Unpolarized and polarized CBET simulations with power balance and pointing variations get the neutron yield correct because both drive energetics and symmetry are important for the yield [Fig. 2(b)]. (3) Both CBET models with power balance and pointing variations match the flow velocity correctly for shot 94712 because the large pointing error dominates the low-mode sources. (4) Polarized CBET with power balance and pointing is needed to get the flow velocity correct for the more-accurately pointed shot 94343 (the low offset of $3.5 \mu\text{m}$ is seen to play a minor role). This indicates that the polarization effect becomes more important as other low-mode sources become smaller. The flow direction is reproduced correctly in all simulations as long as the effects of polarized CBET, beam imbalance, and beam pointing are accounted for. The full comparison to experiments is reported in Ref. 3.

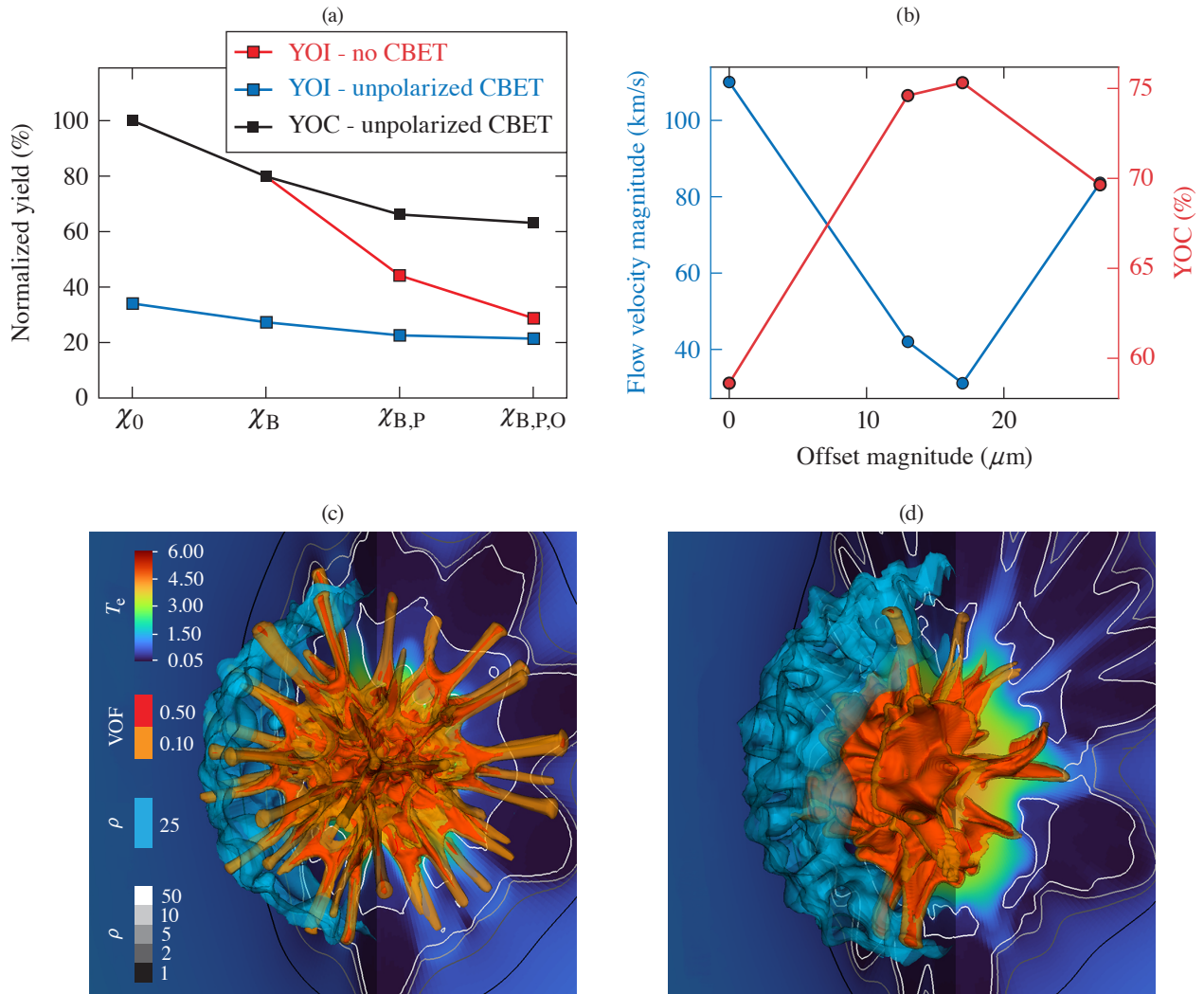


TC16212JR

Figure 2

[(a),(b)] Comparison of the simulated (colored symbols) and measured (gray-shaded areas) (a) peak neutron rise time and (b) neutron yield. Simulations include a variety of low-mode sources and were conducted with and without CBET (see legends). Error bars on the simulated neutron yield account for the effect of small-scale mixing. Experimental yields are corrected for tritium aging.²³

By examining the various simulations, it is observed that these best-setup OMEGA implosions lose $\sim 40\%$ in yield due to effects of balance, pointing, and offset alone [Fig. 3(a)]. In that framework, the polarization effect of CBET causes only a small drop in yield, by about 6%. However, in cases where there is no prior low-mode asymmetry from balance or pointing, the polarized CBET alone reduces the yield by 18% and induces an $\sim 90\text{-km/s}$ flow anomaly compared to an unpolarized CBET case. In addition, the effect of unpolarized CBET alone reduces the yield by $\sim 65\%$ and amplifies the mode-10 anomaly by a factor of 2 to 3, leading to target perforation [Fig. 3(c)]. This is a strong argument for mitigation of the polarized CBET anomaly. It is observed, however, that the yield's dependency on low modes is more severe in cases without CBET because the latter was acting to mitigate drive asymmetries. These results highlight how CBET is a coupling loss mechanism that should be mitigated altogether in future driver designs.



TC161213JR

Figure 3

(a) Scaling of the YOI (yield-over-ideal case in the absence of CBET) and YOC (yield-over-clean case in the presence of CBET) for simulations with and without unpolarized CBET, as a function of low-mode asymmetry sources (cases are labeled with a χ on the x axis; subscript 0 refers to the ideal case; B, P, and O indicate that beam balance, pointing, and offset were accounted for, respectively). (b) Flow anomaly (blue) and YOC (red) as functions of offset magnitude for a case with measured power balance and beam pointing ($\chi_{B,P}$). The target offset is in the opposite direction of the measured flow without offset. [(c),(d)] Target hot-spot electron temperature [colored background (keV)], 10% and 50% volume fraction of DT gas (orange and red volume contours, respectively), 25-g/cm³ density isovalue (light blue volume contour), and 1-, 2-, 5-, 10-, and 50-g/cm³ isocontours (black to white contour lines), for (c) an ideal case (χ_0) with unpolarized CBET. (d) A “real-setup” implosion accounting for power balance and beam pointing ($\chi_{B,P}$), with polarized CBET, is shown for comparison. All figures here relate to shot 94343.

Finally, two mitigation strategies are explored to compensate for the low-mode polarized CBET anomaly: offset compensation and DPR redesign. The offset compensation is able to increase the yield by $\sim 15\%$ [Fig. 3(b)] and reduce the modal $\ell = 1$ anomaly from the polarization effect by a factor of ~ 3 . The offset compensation is not able to further improve the performances, however, due to the presence of other modes, notably from the polarized CBET anomaly but also from pointing and balance errors. Alternatively, considering a design of the DPR with only a 10- μm spot separation and half the smoothing by spectral dispersion (SSD) bandwidth, the simulations show that the flow direction and magnitude anomaly from the polarization effect disappear, and the unpolarized result is recovered. It is noted that halving the SSD bandwidth must be done in consideration of the potential effect on high mode-growth (not modeled here).

This work was granted access to the HPC resources of TGCC under the allocation 2020-A0070506129, 2021-A0090506129 made by GENCI, and PRACE grant number 2021240055. This work has been carried out within the framework of the EUROfusion Consortium, funded by the European Union via the Euratom Research and Training Programme (Grant Agreement No 101052200—EUROfusion). Views and opinions expressed are however those of the author(s) only and do not necessarily reflect those of the European Union or the European Commission. Neither the European Union nor the European Commission can be held responsible for them. The involved teams have operated within the framework of the Enabling Research Project: ENR-IFE.01.CEA “Advancing shock ignition for direct-drive inertial fusion.” The software used in this work was developed in part at the University of Rochester’s Laboratory for Laser Energetics. This material is based upon work supported by the Department of Energy National Nuclear Security Administration under Award No. DE-NA0003856, the University of Rochester, and the New York State Energy Research and Development Authority.

1. A. Colaitis *et al.*, Phys. Rev. Lett. **129**, 095001 (2022).
2. A. Colaitis *et al.*, “3-D Simulations of Implosions in Presence of Low Mode Asymmetries Part 1: Inline Polarized Cross Beam Energy Transfer Modeling,” submitted to Plasma Physics and Controlled Fusion.
3. A. Colaitis *et al.*, “3-D Simulations of Implosions in Presence of Low Mode Asymmetries Part 2: Systematic Flow Anomalies and Low Modes Impact on Performances on OMEGA,” submitted to Plasma Physics and Controlled Fusion.
4. T. R. Boehly *et al.*, Opt. Commun. **133**, 495 (1997).
5. S. P. Regan *et al.*, Bull. Am. Phys. Soc. **66**, CO04.00011 (2021).
6. D. H. Edgell *et al.*, Phys. Rev. Lett. **127**, 075001 (2021).
7. A. Colaitis *et al.*, Phys. Plasmas **26**, 072706 (2019).
8. I. V. Igumenshchev *et al.*, Phys. Plasmas **23**, 052702 (2016).
9. I. V. Igumenshchev *et al.*, Phys. Plasmas **24**, 056307 (2017).
10. A. Colaitis *et al.*, J. Comput. Phys. **443**, 110537 (2021).
11. O. M. Mannion *et al.*, Phys. Plasmas **28**, 042701 (2021).
12. Yu. A. Kravtsov and Yu. I. Orlov, *Caustics, Catastrophes and Wave Fields*, 2nd ed., Springer Series on Wave Phenomena (Springer-Verlag, Berlin, 1993).
13. Yu. A. Kravtsov and N. Y. Zhu, *Theory of Diffraction: Heuristic Approaches*, Alpha Science Series on Wave Phenomena (Alpha Science International Ltd., Oxford, United Kingdom, 2010).
14. A. Colaitis *et al.*, Phys. Plasmas **26**, 032301 (2019).
15. A. B. Langdon, Phys. Rev. Lett. **44**, 575 (1980).
16. I. V. Igumenshchev *et al.*, Phys. Plasmas **17**, 122708 (2010).
17. J. A. Marozas *et al.*, Phys. Plasmas **25**, 056314 (2018).
18. D. H. Edgell *et al.*, Phys. Plasmas **24**, 062706 (2017).
19. R. K. Follett *et al.*, Phys. Rev. E **98**, 043202 (2018).
20. P. Michel *et al.*, Phys. Plasmas **16**, 042702 (2009).
21. L. Spitzer, Jr. and R. Härm, Phys. Rev. **89**, 977 (1953).
22. D. Turnbull *et al.*, Phys. Rev. Lett. **124**, 185001 (2020).
23. A. Lees *et al.*, Phys. Rev. Lett. **127**, 105001 (2021).